



Published in final edited form as:

Biochemistry. 2011 November 8; 50(44): 9421–9423. doi:10.1021/bi201487b.

Neutron structure of human carbonic anhydrase II: A hydrogen bonded water network “switch” is observed between pH 7.8 and 10.0

Zoë Fisher[✦], Andrey Y. Kovalevsky[✦], Marat Mustyakimov[✦], David N. Silverman^{||}, Robert McKenna[§], and Paul Langan[‡]

[✦]Bioscience Division, Los Alamos National Laboratory, Los Alamos NM 87544

[§]Dept. of Biochemistry and Molecular Biology, University of Florida, Gainesville FL 32611

^{||}Department of Pharmacology and Therapeutics, University of Florida, Gainesville FL 32611

[‡]Center for Structural Molecular Biology, Oak Ridge National Laboratory, Oak Ridge TN 37831

Abstract

The neutron structure of wild type human carbonic anhydrase II at pH 7.8 has been determined to 2.0 Å resolution. Detailed analysis and comparison to the previously determined structure at pH 10.0 shows important differences in protonation of key catalytic residues in the active site as well as a rearrangement of the hydrogen bonded water network. For the first time, a completed hydrogen bonded network stretching from the Zn-bound solvent to the proton shuttling residue His64 has been directly observed.

Keywords

neutron diffraction; hydrogen bond; carbonic anhydrase; deuterium; proton transfer

Human carbonic anhydrase II (HCA II) is a 29 kDa monomeric Zn-metalloenzyme that catalyzes the reversible hydration of CO₂ into HCO₃⁻ and a proton, and is found prominently in red blood cells and secretory tissues. HCA II is one of the fastest enzymes known with a *k*_{cat} for CO₂ hydration of 106/sec and its activity is close to diffusion limited (1). HCA II serves as a relatively simple model enzyme for the study of long-range proton transfer mechanisms in more complex systems, such as ATP synthase, bacteriorhodopsin, and cytochrome *c* oxidase. There is also increasing industrial interest in using engineered carbonic anhydrase for carbon dioxide extraction from flue gas in coal-fired power plants (2). Analyses of HCA II neutron structures provide unique data and insights into proton transfer mechanisms and could have broad applicability to many other systems.

All CAs identified to date use a metal-hydroxide mechanism to mediate the two-step ping-pong catalytic mechanism (3). The first step of catalysis by HCA II is a nucleophilic attack on incoming CO₂ by a Zn-bound OH⁻ to produce HCO₃⁻. The binding of HCO₃⁻ at the metal is weak and accordingly is easily displaced by a water molecule. The second step

^{*}Corresponding Author: S. Zoë Fisher. zfisher@lanl.gov; Phone (505) 665-4105.

SUPPORTING INFORMATION.

Details of crystallization, data collection, and structure refinement; crystallographic data table for both room temperature neutron and X-ray diffraction data. Additional figures of waters, His64, and active site. This material is available free of charge via the Internet at <http://pubs.acs.org>. Structural coordinates and experimental data have been deposited in the Protein Data Bank as PDB ID 3TMJ.

activates the metal-bound water to OH^- through a series of proton transfers (1, 4). This is thought to occur through a network of well-ordered H-bonded waters (4, 5). This network stretches from the metal to the proton shuttling residue, His64, and is H-bonded to several hydrophilic residues that line the active site (Figure S1; 6, 7). In structural studies residue His64 has been observed to occupy two distinct positions, termed the inward and outward conformations, pointing towards and away from the Zn active site, respectively (8, 9). Exactly how protons move in the active site of proteins is not clear but it has been proposed that a Grotthus proton hopping mechanism or the formation of a series of Zundel (H_5O_2^+) or Eigen cations (H_9O_4^+) may be factors (10). It has been postulated that the inward conformation of His64 might be poised to accept the excess proton from the water network, while the outward conformation is ready for proton shuttling to the bulk solvent. This observed flexibility of His64 is most likely related to its protonation state (7, 11). The enzyme displays very strong pH dependence for both k_{cat} and $k_{\text{cat}}/K_{\text{M}}$ that are defined by a single ionization corresponding to a pK_{a} of ~ 7 (1).

The details of CO_2 binding and subsequent hydration are clearer since the structure determination of CO_2 at the active site revealed a side-on binding coordination (12). Currently neutron crystallography studies on HCA II have focused on the structural details of the active site hydrophilic residues and water molecules involved in proton transfer. As such the analysis of the neutron structure at high pH ($\sim \text{pH } 10$) has been previously reported (13).

The approach taken in the current study was to change the pH of the crystal as a way to modulate the changes in protonation that occur during catalysis. Discussed here is the pH 7.8 crystal structure that is compared to the previously determined pH 10.0 form. The advantage of neutron crystallography is that H and its isotope D diffract neutrons very strongly and to about the same extent as the heavier atoms found in proteins such as N, C, or O (scattering lengths in fm: H = -3.74 , D = 6.67 , N = 9.4 , C = 6.6 , O = 5.8). Accordingly, H and D atoms appear as negative or positive peaks, respectively, in nuclear scattering density maps. In this study the crystal was subject to H/D vapor exchange, to replace labile H with D, thus promoting strong positive scattering from D atoms. The benefit of using vapor exchange instead of soaking is that there is less chance of damage to the large crystals required for neutron studies. Using neutron diffraction on H/D exchanged samples it is possible, even at medium ($2.0 - 2.2 \text{ \AA}$) resolution, to directly observe the protonation states of amino acid residues (eg. neutral vs. charged histidine residues) and to distinguish between D_3O^+ , D_2O , and OD^- (14,15). The room temperature neutron structures were complemented with X-ray data from a similar crystal prepared and H/D exchanged in the same manner. Using the joint neutron and X-ray methodology for model refinement leads to more accurate structures in that X-rays provide highly accurate information for the heavier atoms in proteins while neutrons are used to refine the positions of H/D atoms, effectively increasing the data-to-parameter ratio for refinement. In this way the data are highly complementary and allow a detailed understanding of hydration and H-bonding in proteins (16).

Careful analyses of omit and difference nuclear density maps revealed several interesting features in the pH 7.8 structure that are different from those at high pH. The most interesting one - from a proton transfer point of view - is that the water network has rearranged in response to the reduced pH and forms a completed hydrogen bonded network between the Zn-bound solvent (ZW) and W2 not observed before (Figure 1).

At high pH, W1 was acting as an H-bond donor to the Zn-bound water (ZW) and Thr200 (left panel in Figure 1). In this configuration there is a break in the H-bonded water network between W1 and W2. This can, in part, explain the lower observed rate constant for proton transfer between His64 and the zinc-bound solvent molecule. At pH 7.8 of the current

structure, the positions of the water termed “Deep Water” (DW) because of its location in the active site and ZW are unchanged. However, W1 has flipped to engage in an H-bond to W2 and now acts as an H-bond acceptor to Thr200 (right panel in Figure 1). Accordingly, W2 and W3a have changed orientation in a compensatory manner to remain H-bonded to each other and W1. This rearrangement positions one of the W2 D atoms to act as an H-bond donor to His64 (right panel Figure 1). This represents an unbranched proton transfer pathway between ZW and His64, something that is thought to be essential for efficient proton transfer (17). Previous computational studies have implied that proton transfer occurs through W3a, but this observation supports the notion that proton transfer most likely occurs through W2 (11). It also provides a clue to the specific participation of an explicit water molecule in proton transfer. The cluster of H-bonds between W3b, Asn62, and Asn67 are completely unchanged from the high pH structure. Table 1 shows the O...O distances and O-D...O H-bond donor acceptor angles between waters in the pH 10 and 7.8 structures. Within the structural coordinate errors at 2.0 Å resolution, the O distances are identical while the D atoms rearrange.

The fact that the solvent O positions are unchanged while only the D atoms are re-organizing is consistent with the significant role of the hydrophilic residues of the active site, such as Asn62 and Asn67, in stabilizing the positions of water molecules in the structure. The change in H-bonding of the water structure is most likely due to the significant changes in the charged states of two key residues, Tyr7 and His64, demonstrating the effect of changing electrostatics in the active-site cavity. An unanticipated result observed in the high pH structure was that Tyr7 was deprotonated, implying that this residue has a lower pK_a than that for free Tyr in solution (Figure 2) (13).

As anticipated Tyr7 is indeed protonated at pH 7.8 (Figure 2) but it was thought that it would still act as H-bond acceptor from W3a and that the phenolic D atom would point towards the buried water W1003 (13). Instead, at pH 7.8 Tyr7 OD makes a bifurcated H-bond to buried water W1003 and W3a (Figure 2). The O...O distances between the phenolic O of Tyr7 to W1003 and W3a are 2.6 Å each. This significant electrostatic change from the negatively charged deprotonated oxygen to neutral protonated OD group may be causing W3a to flip and establish an H-bond with W2 (Figures 1–3). This, along with the changes observed in His64, is causing a cascade of flipping and re-establishing of H-bonds along the water network. This raises interesting implications for Tyr affecting proton transfer at high pH *in vitro*, such as the possibility that Tyr7 may act as a proton trap at high pH.

As expected, at high pH His64 was observed to be neutral and in a single inward conformation. At pH 7.8 His64 occupies three superimposed forms: the predominant one is neutral (~60% occupancy), another one is flipped and neutral (~30% occupancy, Figure S3), and finally we observed a minor flipped charged species (~10% occupancy, not shown). The predominant form directs the Nδ1 electron lone pair toward W2's D atom, indicating formation of an H-bond between W2 and His64 (Figure 3). The orientations of the 30% neutral and the minor protonated form, with their rings flipped ~180°, are similar to that observed for the neutral imidazole ring at high pH. The observation of the minor protonated species is consistent with the pK_a of His64 as ~ 7 considering the pH of the crystal (pH 7.8).

These observations reveal important contributions to the understanding of the molecular details of proton transfer in HCA II. A change in pH in the crystals has permitted the observation of what might happen during catalysis. This has allowed the observation, for the first time, of a completed H-bonded network connecting the ZW to His64. In addition, His64 was observed in an intermediate state where a minor form is protonated, possibly poised to rotate to the outward conformation to deliver the excess proton to the bulk solvent.

To further probe the role of Tyr7 during catalysis ¹³C-labeled Tyr HCA II is being prepared for pH titrations using NMR to look at the pKa of all 7 Tyr and the active pursuit of a low pH crystal form to shed more structural light on proton transfer.

Supplementary Material

Refer to Web version on PubMed Central for supplementary material.

Acknowledgments

Funding Sources

The PCS is funded by the Office of Biological Environmental of the U.S. Dept. of Energy. SZF is partially funded by LANL LDRD Early Career grant # 20110535ER. PL and MM are partially funded by NIH-NIGMS GM071939. RM and DNS are partially funded through NIH-NIGMS GM25154.

ABBREVIATIONS

HCA II	human carbonic anhydrase II
H-bond	hydrogen bond
PCS	Protein Crystallography Station

References

1. Silverman DN, Lindskog S. *Acc Chem Res.* 1988; 21:30–36.
2. Favre N, Christ ML, Pierre AC. *J Mol Cat B: Enzymatic.* 2009; 60:163–170.
3. Christianson DW, Fierke CA. *Acc Chem Res.* 1996; 29:331–339.
4. Silverman DN, McKenna R. *Acc Chem Res.* 2007; 40:669–675. [PubMed: 17550224]
5. Venkatasubban KS, Silverman DN. *Biochemistry.* 1980; 19:4984–4989. [PubMed: 6779860]
6. Tu CK, Silverman DN, Forsman C, Jonsson B-H, Lindskog S. *Biochemistry.* 1989; 28:7913–7918. [PubMed: 2514797]
7. Fisher SZ, Tu CK, Bhatt D, Govindasamy L, Agbandje-McKenna M, McKenna R, Silverman DN. *Biochemistry.* 2007; 46:3803–3813. [PubMed: 17330962]
8. Nair SK, Christianson DW. *J Amer Chem Soc.* 1991; 113:9455–9458.
9. Fisher SZ, Hernandez-Prada J, Tu CK, Duda D, Yoshioka C, An H, Govindasamy L, Silverman DN, McKenna R. *Biochemistry.* 2005; 44:1097–1105. [PubMed: 15667203]
10. Davidson VL. *Nature Chem.* 2011; 3:662–663. [PubMed: 21860447]
11. Maupin CM, McKenna R, Silverman DN, Voth GA. *J Amer Chem Soc.* 2009; 131:7598–7608. [PubMed: 19438233]
12. Domsic JF, Avvaru BS, Kim CU, Gruner SM, Agbandje-McKenna M, Silverman DN, McKenna R. *J Biol Chem.* 2008; 382:30766–30771. [PubMed: 18768466]
13. Fisher SZ, Kovalevsky AY, Domsic JF, Mustyakimov M, McKenna R, Silverman DN, Langan PA. *Biochemistry.* 2010; 49:415–421. [PubMed: 20025241]
14. Kovalevsky AY, Hanson BL, Mason SA, Yoshida T, Fisher SZ, Mustyakimov M, Forsyth VT, Blakeley MP, Keen DA, Langan PA. *Angew Chem Int Ed.* 2011; 50:7520–7523.
15. Kovalevsky AY, Katz AK, Carrell HL, Hanson L, Mustyakimov M, Fisher SZ, Coates L, Schoenborn BP, Bunick GJ, Glusker J, Langan P. *Biochemistry.* 2008; 47:7595–7597. [PubMed: 18578508]
16. Adams PD, Mustyakimov M, Afonine PV, Langan PA. *Acta Cryst D.* 2009; 65:567–573. [PubMed: 19465771]
17. Cui Q, Karplus M. *J Phys Chem B.* 2003; 107:1071–1078.

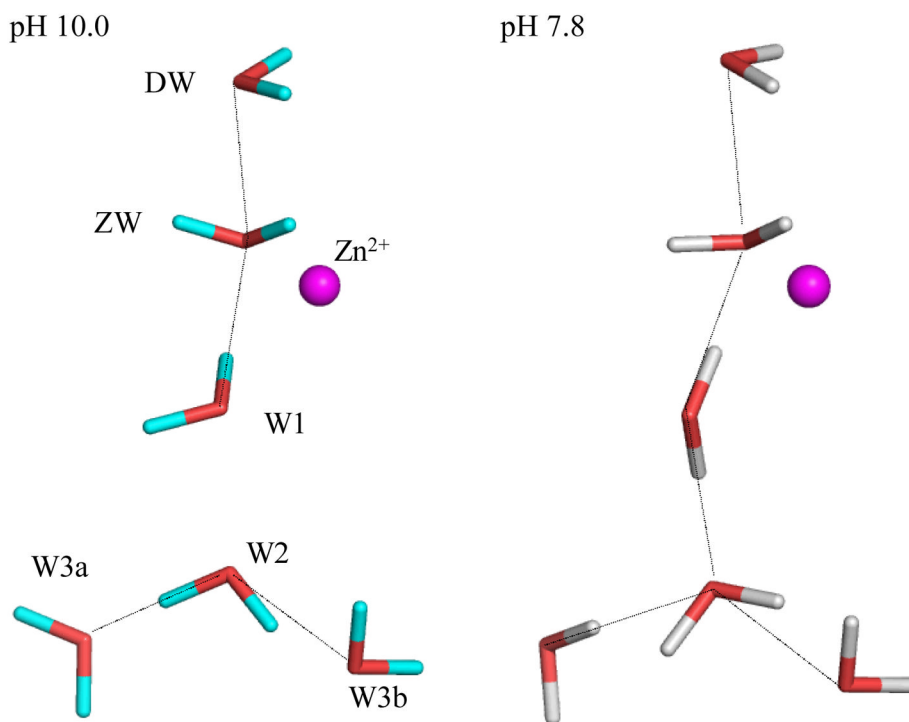


Figure 1. Comparison stick diagram of the water networks in the active site of HCA II determined by neutron crystallography at pH 10 (left) and 7.8 (right). Zn is included for reference and waters are as labeled. Observed hydrogen bonds are shown as black lines, active site amino acid residues are omitted for clarity.

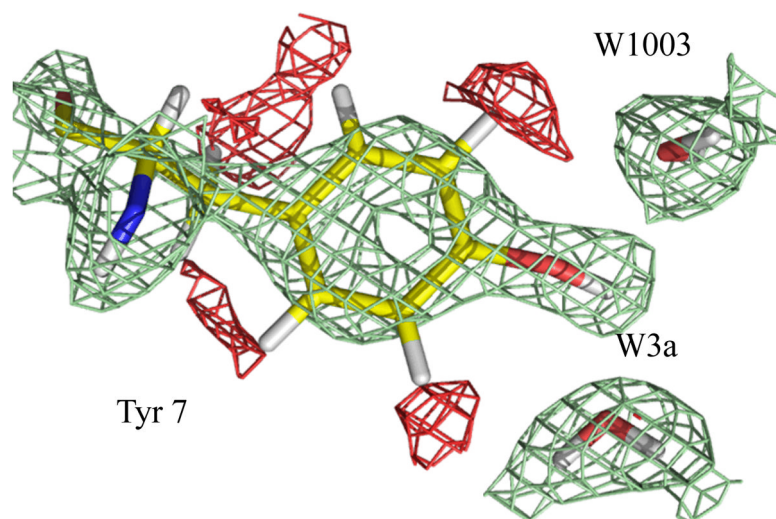


Figure 2. Tyr7 protonated in the pH 7.8 structure, and can act as a bifurcated H-bond donor to W3a and W1003. Positive $2F_o - F_c$ nuclear maps are shown in green (contoured at 1.5s) with the negative $2F_o - F_c$ nuclear map shown in red (contoured at 2.0s), indicating the unexchanged/non-labile H density.

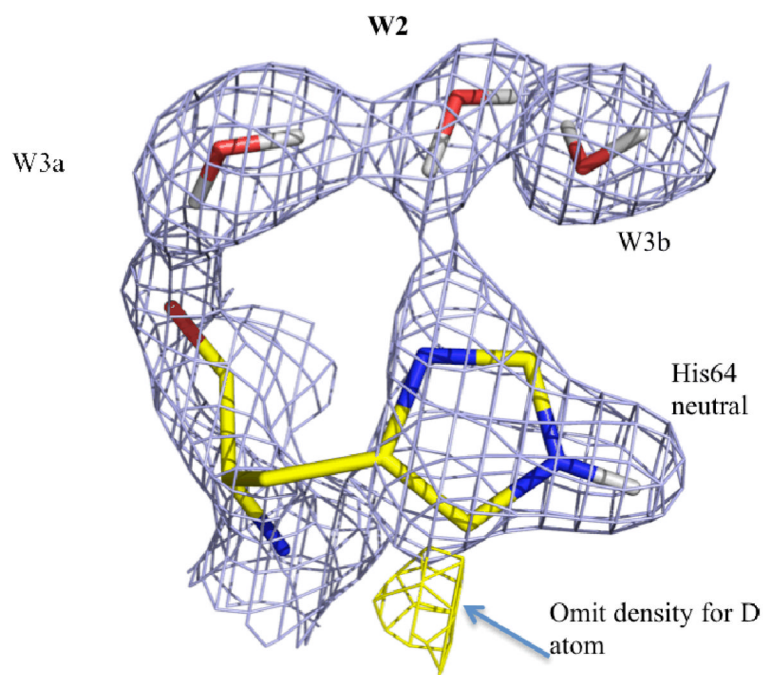


Figure 3. The predominant conformation of the His64 side chain is neutral and in the “inward” position. The $2F_o - F_c$ nuclear map (contoured at 1.5σ) is shown in blue with the positive omit $F_o - F_c$ nuclear density map (contoured at 3.0σ) in yellow, indicating the D atom density for the flipped neutral histidine conformation. Waters are as labeled, H atoms on the His imidazole ring are omitted for clarity.

TABLE 1

Table shows O...O distances and angles between H-bond donor-acceptors for the water networks determined at pH 10 and pH 7.8.

pH 10.0	O...O in Å (O-D...O in °)	pH 7.8	O...O in Å (O-D...O in °)
W1-ZW	2.5 (170)	W1-ZW	2.7 (170)
W1-W2	2.8 (n/a)	W1-W2	2.7 (170)
W2-W3a	2.7 (150)	W3a-W2	2.9 (150)
W2-W3b	2.8 (160)	W2-W3b	2.7 (170)